

Use of Molecular Scaffolding for the Stabilization of an Intramolecular Dative P^{III} - P^V System

Petr Kilian,^[a] Douglas Philp,^[a] Alexandra M. Z. Slawin,^[a] and J. Derek Woollins*^[a]

Keywords: Phosphorus heterocycles / Strained molecules / Neighbouring-group effects / Phosphorus–phosphorus bond

The reaction of NapP_2S_4 (**1**; Nap = naphthalene-1,8-diyl) with chlorine gas gave $[\text{Nap}(\text{PCl}_2)(\text{PCl}_4)]$ (**2**), displaying a rare $\sigma^4\text{P}-\sigma^6\text{P}$ bonding interaction. An X-ray structure analysis confirmed the PCl_5 -like, P–P bond containing phosphonium-phosphoride structure of **2** in the crystal, which was also found in solution at low temperature. At ambient and higher temperatures, dynamic behaviour on the NMR time-scale was observed, which was assigned to interchange of the ionic phosphonium-phosphoride form **2** and the molecular bis(phosphorane) $\text{Nap}(\text{PCl}_3)_2$ form **3**, rather than to the ionic phosphonium salt-phosphorane form $[\text{Nap}(\text{PCl}_3)(\text{PCl}_2)][\text{Cl}]$ **4**. Electronic structure calculations were performed at the

B3LYP/6–31G(d,p) level of theory on structures **2** and **3**; structure **3** was located as a local minimum on the potential energy surface, 15 kcal·mol^{−1} higher in energy than structure **2**. The crystal structure and calculated P–P distances are 2.34 and 2.31 Å for **2** and **3**, respectively. An activation energy of 19.7 kcal·mol^{−1} was found for the transition state structure by coordinate driving calculations; the line-shape analysis of variable temperature $^{31}\text{P}\{^1\text{H}\}$ NMR spectra gave an activation energy of 14.4 kcal·mol^{−1}.

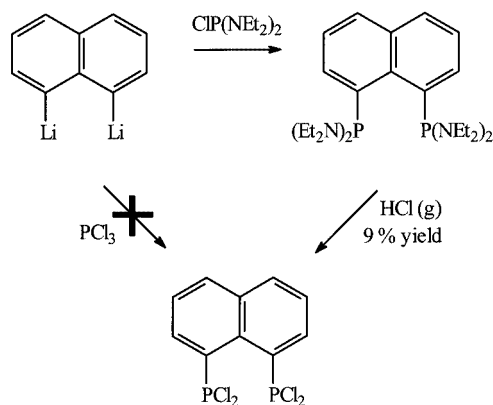
(© Wiley-VCH Verlag GmbH & Co. KGaA, 69451 Weinheim, Germany, 2003)

Introduction

Sterically overcrowded and therefore structurally distorted molecules or molecular ions have attracted the attention of chemists for many years. Bay region substituted polycyclic aromatic hydrocarbons, such as 1,8-disubstituted naphthalenes, are one of the most intensively studied systems in this field. The rigidity of the naphthalene backbone combined with the close proximity of functional groups in these species offer an ideal scaffolding for unusual chemistry as well as interesting bonding and geometry.

In the case of 1,8-diphospha-substituted naphthalenes, NapP_2S_4 (**1**, Nap = naphthalene-1,8-diyl) has been widely used as a synthon,^[1–3] however there is an obvious lack of further suitably versatile, easily accessible starting materials, such as $\text{Nap}(\text{PCl}_2)_2$ or $\text{Nap}(\text{PH}_2)_2$. Halophosphoranes and halophosphanes are especially valuable synthons in organophosphorus chemistry. The preparation of the most desirable derivative $\text{Nap}(\text{PCl}_2)_2$ has been published recently.^[4] As the direct method of preparation from lithiated naphthalene (NapLi_2) and PCl_3 was not successful (Scheme 1), protection was employed. Thus the reaction of NapLi_2 and protected chlorophosphane, followed by deprotection (Scheme 1) gave the desired $\text{Nap}(\text{PCl}_2)_2$. Formation of stable intermediates in the deprotection step, though, resulted in a low overall yield, which seems to restrain broader synthetic use of this method. In the search for fur-

ther methods for the preparation of halogenated 1,8-diphosphanaphthalene synthons, we have obtained a new derivative $\text{Nap}(\text{PCl}_4)(\text{PCl}_2)$ **2**, which is not only a promising synthon, but also contains a very rare $\sigma^4\text{P}-\sigma^6\text{P}$ bond as well as showing interesting fluxionality on the NMR timescale.



Scheme 1. Route to $\text{Nap}(\text{PCl}_2)_2$ via NapLi_2

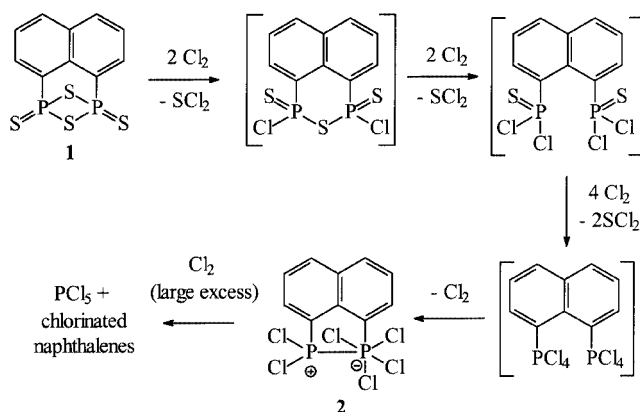
Results and Discussion

Synthesis

The reaction of NapP_2S_4 **1** with a slight excess of chlorine gas proceeded with complete desulfuration, yielding the yellow solid $\text{Nap}(\text{PCl}_4)(\text{PCl}_2)$ **2** (Scheme 2). A plausible mechanism for the chlorination involves consequential meta-

^[a] School of Chemistry, University of St. Andrews, St. Andrews, Fife, KY16 9ST, United Kingdom
E-mail: jdw3@st-andrews.ac.uk

thesis of a) bridging and b) terminal sulfur atoms, leading to the bis(phosphorane) $\text{Nap}(\text{PCl}_4)_2$. The next step — a spontaneous elimination of Cl_2 from $\text{Nap}(\text{PCl}_4)_2$ with formation of **2** — is obviously a consequence of the excessive steric strain connected with such an overcrowded molecular geometry: $\text{Nap}(\text{PCl}_4)_2$ would contain two five-coordinate P atoms kept in close proximity by the rigid organic backbone causing extensive shielding of the coordination sphere of each P atom. Instead of back formation of $\text{Nap}(\text{PCl}_4)_2$, a simultaneous P–P and P–C bond cleavage leading to PCl_5 and chlorinated naphthalenes on prolonged chlorination was observed by ^{31}P and ^1H NMR spectroscopy.



Scheme 2. Reaction of NapP_2S_4 (**1**) with chlorine gas; undetected intermediates are in square brackets

The purification of the crude product **2** was performed by subliming off the major by-product (PCl_5) and further volatiles, followed by twofold recrystallisation from hot THF, resulting in a moderate yield 20% of pure **2**. The oxidation state of the phosphorus atoms in **2** is +4, thus the formation of **2** represents a formal reduction of P^{V} to P^{IV} .

X-ray Investigations

A single crystal X-ray structure determination (Figure 1, Table 1) proved the phosphonium-phosphoride structure of **2** in the crystal. Compound **2** possesses approximate C_s symmetry, with the carbon atoms of the naphthalene backbone, the two P atoms as well as Cl(4) and Cl(6) forming a nearly ideal plane (mean deviation of 0.02 Å) with atoms Cl(6) and P(1) lying only 0.05 Å above and below this plane; the dihedral angle $\text{P}(1)\text{--C}(1)\cdots\text{C}(9)\text{--P}(2)$ is 2° . The P–P interaction in **2** is clearly attractive, the P–P bond length (2.34 Å) is slightly shorter than the peri-separation [$\text{C}(1)\cdots\text{C}(9)$ distance] of 2.51 Å in the organic backbone. It is only very recently that the first examples of P–P bonding interaction ($\sigma^3\text{P}\text{--}\sigma^4\text{P}^+$ type) in 1,8-P,P-naphthalenes were described.^[5] The vast majority of nonbridged 1,8-P,P-naphthalenes show significantly longer $\text{P}\cdots\text{P}$ distances, twisting of the naphthalene ring and distortions of the *ipso*-C geometries as a result of repulsive $\text{P}\cdots\text{P}$ interactions. For example, no evidence of a $\text{P}\cdots\text{P}$ attractive interaction (e.g.

ative bond) was found in the phosphonium salts **A** (Figure 2, $\text{P}\cdots\text{P}$ distances: 3.19 and 3.26 Å), where the P environments are similar to those in **2**.^[6] Compound **2** thus represents only the second type of attractive P–P interaction in 1,8-P,P-naphthalenes proved by means of a single crystal X-ray structure determination.

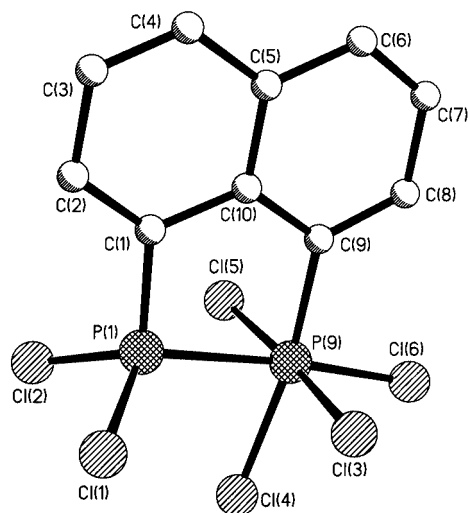


Figure 1. Crystal structure of **2** (H atoms omitted for clarity); for selected bond lengths and angles see Table 1

Table 1. Comparison of selected bond lengths [Å] and angles [$^\circ$] for the crystal structure of **2** and calculated [B3LYP/6–31G(d,p)] structures **2** and **3**

	2 (X-ray)	2 (calcd.)	3 (calcd.)
P(1)–P(9)	2.338(2)	2.390	2.313
P(1)–C(1)	1.755(4)	1.755	1.904
P(9)–C(9)	1.883(4)	1.883	1.800
P(1)–Cl(1)	1.988(2)	1.995	2.075
P(1)–Cl(2)	1.978(2)	1.995	2.075
P(9)–Cl(3)	2.164(2)	2.162	2.216
P(9)–Cl(4)	2.178(2)	2.160	–
P(1)–Cl(4)	–	–	2.277
P(9)–Cl(5)	2.149(2)	2.158	2.216
P(9)–Cl(6)	2.088(2)	2.082	2.077
C(1)–C(10)	1.422(6)	1.430	1.429
C(9)–C(10)	1.425(6)	1.431	1.430
C(1)–P(1)–P(9)	99.7(2)	99.0	85.9
C(9)–P(9)–P(1)	86.1(1)	84.8	98.9
C(10)–C(1)–P(1)	111.6(3)	112.8	119.9
C(10)–C(9)–P(9)	118.4(3)	120.4	112.5
C(1)–C(10)–C(9)	124.0(4)	123.1	122.8

The P–P distance of 2.34 Å in **2** lies near to the upper limit of the range for P–P single bonds (2.20–2.35 Å) and is the longest observed for $\sigma^4\text{P}\text{--}\sigma^6\text{P}$ bonds reported to date [range 2.165–2.2962(6) Å].^[7,8] The rather long P–P bond length may be accounted for by: i) a released, but still significant, strain in the structure of **2** (indicated by angular distortions of both P environments), ii) a mismatch between the optimal P–P bond length and the peri separation on

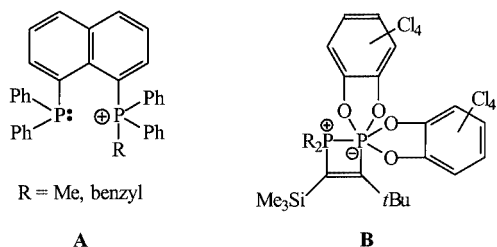


Figure 2. Structural formula of phosphonium salts **A** and $\sigma^4\text{P} \rightarrow \sigma^6\text{P}$ ylide **B**; non-coordinating counteranions were present in salts **A**

the naphthalene skeleton, and iii) the lower basicity of the organo- PCl_2 group compared, for example, to the trialkylphosphanyl group. The P(1) environment is distorted tetrahedral [C(1)–P(1)–P(9) angle $99.7(2)^\circ$], whilst the P(9) environment is distorted octahedral [C(9)–P(9)–Cl(6) angle $99.1(2)^\circ$]. As expected, the P–Cl bond lengths of the four-coordinate P(1) atom are shorter than these of the six-coordinate P(9) atom [1.978(2)–1.988(2) vs. 2.088(2)–2.178(2) Å]. It should be noted that **2** represents a rare examples of an organochlorophosphorane having a solid-state structure similar to that of solid $[\text{PCl}_4][\text{PCl}_6]$.^[9]

From the few examples of the donor type $\sigma^4\text{P} \rightarrow \sigma^6\text{P}$ linkage known,^[7,8,10–13] it can be concluded that a strong donor-acceptor interaction is required for its stabilisation. This interaction is facilitated by both the high Lewis acidity and the basicity of the $\sigma^6\text{P}$ and $\sigma^4\text{P}$ atoms, respectively, which are dictated by the electron-withdrawing or -donating nature of the substituents. As the organo- PCl_2 group in **2** cannot be regarded as a strong donor, the release of the steric strain by formation of a P–P bond and the coherent transformation of the naphthalene ring into a planar geometry is probably the important factor contributing to the stabilisation of the unusual $\sigma^4\text{P} \rightarrow \sigma^6\text{P}$ bond in **2**. Indeed, a similar “scaffolding” mechanism was found to play an important role in the stabilisation of unusual P–P interactions (including $\sigma^4\text{P} \rightarrow \sigma^6\text{P}$) in the unsaturated four-membered ring skeleton **B** (Figure 2).^[11]

NMR Investigations and Study of the Equilibrium Processes

The $^{31}\text{P}\{^1\text{H}\}$ NMR spectrum of **2** at 303 K ($[\text{D}_8]\text{THF}$, 109.4 MHz) indicated a dynamic behaviour on the NMR timescale. The spectrum consists of two broad doublets (AX system, $\delta_{\text{P}} = 82.9$ and -225.9 ppm; $^1J_{\text{P,P}} = 118.5$ Hz). At low temperature (213 K) the two doublets sharpen ($\delta_{\text{P}} = 82.9$ and -227.9 ppm; $^1J_{\text{P,P}} = 88.3$ Hz). Such a spectrum results from an ionic phosphonium-phosphoride structure; the chemical shifts are similar to those of PCl_4^+ ($\delta_{\text{P}} = 86$ ppm) and PCl_6^- ($\delta_{\text{P}} = -290$ ppm) as well as to those observed in the solid state ^{31}P MAS spectrum of ionic $[\text{P}(\text{CH}_2\text{Cl})\text{Cl}_3][\text{P}(\text{CH}_2\text{Cl})\text{Cl}_5]$ ($\delta_{\text{P}} = 111$ and -206 ppm).^[9] The relatively small magnitude of the $^1J_{\text{P,P}}$ coupling observed in **2** is not without precedent, a similar magnitude of 122 Hz was observed in a diphosphate^[8] containing a $\sigma^4\text{P}-\sigma^6\text{P}$ bond with a slightly shorter P–P bond length of 2.30 Å. Both the linewidth and $^1J_{\text{P,P}}$ increase substantially

with temperature, only subtle δ_{P} changes were observed (Figure 3). At temperatures higher than 303 K the linewidth is so high that a determination of $^1J_{\text{P,P}}$ is impossible; at 333 K ($[\text{D}_8]\text{THF}$) approximate coalescence temperature was reached, as virtually no ^{31}P resonances were observed.

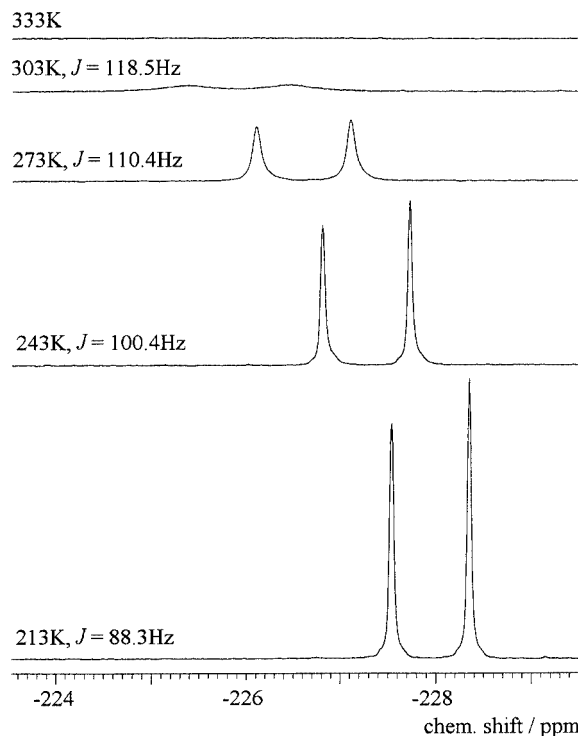


Figure 3. Variable temperature $^{31}\text{P}\{^1\text{H}\}$ NMR spectra (109.4 MHz) of a saturated solution of **2** in $[\text{D}_8]\text{THF}$; high-field half spectrum region is shown, 1024 scans for each temperature; the same line shapes were observed in the low-field half spectrum region

Considerable theoretical and stereochemical interest is attached to phosphorus pentahalides and their organo-substituted relatives because of the variety of structures they adopt. There are three possible structures available for the R_2PCl_3 organochlorophosphoranes, these being ionic $[\text{R}_2\text{PCl}_2][\text{R}_2\text{PCl}_4]$ (like PCl_5), molecular pseudo-trigonal bipyramidal R_2PCl_3 (like PF_5) and ionic phosphonium salt $[\text{R}_2\text{PCl}_2][\text{Cl}]$ (like PBr_5). The relevant bisfunctional equivalents to these structures are depicted in Figure 4, compound **2** representing an intramolecular equivalent of the PCl_5 -like structure. This structure (**2**) has been found both in the solid state and in solution at low temperatures. In order to explain the NMR fluxionality observed at ambient and higher temperatures described above, the interchange between **2** and **3** or **4** may thus be considered (Figure 4).

The interchange between **2** and **4** would involve the presence of Cl^- in the solution. Measurement of the ^{35}Cl NMR spectra of a solution of **2** ($[\text{D}_8]\text{toluene}$, 49.0 MHz, 298 K, 45000 scans) showed no evidence for the presence of Cl^- ions, and thus mitigated against the presence of **4** under these conditions.

Further uncertainty about the presence of **4** in the system arises from the unexpected features found in the ^{31}P NMR spectra of an equilibrium mixture with respect to those of

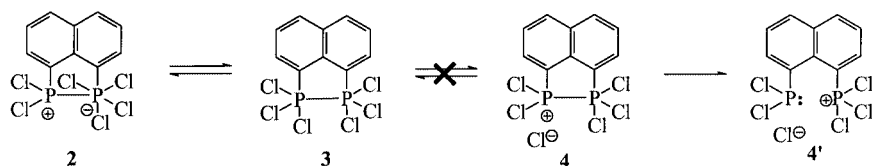


Figure 4. Possible equilibrium structures in solution at ambient and higher temperatures; **2**: ionic phosphonium phosphoride; **3**: molecular bis(pseudo-trigonal bipyramidal); **4**: ionic phosphonium salt-phosphorane; **4'**: ionic phosphanyl-phosphonium salt

the isostructural phosphonium salts **A** (Figure 2). The NMR and X-ray data of **A** (Figure 2) were discussed recently^[6] and we assume that some parallels between phosphonium salts **A** and **4** can be drawn. The X-ray data show that there is no $P \rightarrow P^+$ bonding interaction in **A**. The NMR spectroscopic data of **A** are consistent with this (although dynamic behaviour was observed due to hindered rotation), the magnitudes of $J_{P,P}$ (27–32 Hz) observed were too small for a conventional P–P bond. Although there are differences in the electronegativities of the substituents in **4** and **A**, we expect repulsive P–P interaction in **4**, the more precise description of bonding thus being **4'** (Figure 4). The measurement of a VT $^{31}P\{^1H\}$ NMR spectrum of a solution of **2** showed an increase of the magnitude of $J_{P,P}$ with increasing temperature (Figure 3). The preservation of $^1J_{P,P}$ at higher temperatures indicates that the P–P bond is retained throughout. This behaviour is obviously inconsistent with the $P \cdots P$ nonbonding interaction in **4'**, providing further support that **3** is involved.

In order to gain further insight into the equilibrium processes depicted in Figure 4, we performed electronic structure calculations on structures **2** and **3** at the B3LYP/6–31G(d,p) level of theory. The calculated structures are shown in Figure 5. The geometry around the two P centres in **2** is reproduced well by the calculations (Table 1). Structure **3** was located as a local minimum on the potential energy surface 15 kcal·mol^{−1} higher in energy than structure **2**. A shorter P–P bond length (2.31 Å) was found in **3**. Although both σ^5P environments in **3** are approximately trigonal bipyramidal, and the phosphorus atoms lie in the plane of the naphthalene ring, they are not related by any symmetry element in the molecule. In the trigonal bipyramidal geometry of P(1) the C(1) and Cl(4) atoms are axial, whereas in the trigonal bipyramidal geometry of P(9), Cl(3) and Cl(5) occupy the axial positions.

This result again demonstrates the stabilisation of an unusual bonding geometry in peri-substituted naphthalenes. Up to now, only two X-ray structures of compounds containing a σ^5P – σ^5P bond have been reported, in which the P–P bond was axial^[14] and equatorial.^[15,16]

In order to further assess the fluxional behaviour of **2**, we performed coordinate driving calculations in which one chlorine atom from the octahedral P centre was transferred in a concerted manner to the tetrahedral P centre, thus converting **2** into **3**. The calculations indicated that these interconversions are plausible and a transition state structure (Figure 6) is obtained for the axial chlorine [Cl(4)] transfer

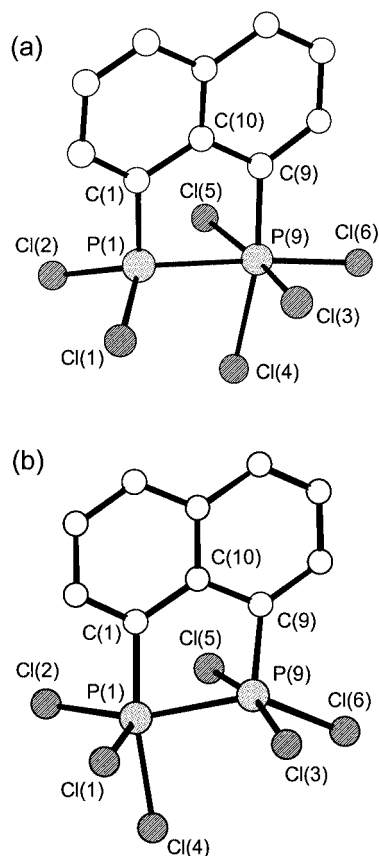


Figure 5. Calculated [B3LYP/6–31G(d,p)] structures of: (a) compound **2**, and (b): compound **3** (H atoms omitted for clarity); for selected bond lengths and angles see Table 1

pathway. The calculated activation energy is 19.7 kcal·mol^{−1} for the conversion of **2** to **3**.

The approximate activation energy of 14.4 kcal·mol^{−1} was found by line shape analysis of the variable temperature $^{31}P\{^1H\}$ NMR spectra, using the expression $k = \pi(\Delta\nu)$, where $\Delta\nu$ is the difference (Hz) between the line width at a temperature T , where exchange of sites is taking place (273 K), and the line width in the absence of exchange (183 K). The Eyring equation was subsequently employed to calculate the ΔG^\ddagger value at T . The values obtained independently from NMR spectroscopic data and coordinate driving calculations show good agreement; the relatively high barrier probably reflects the significant shortening of the P–P distance in the transition state.

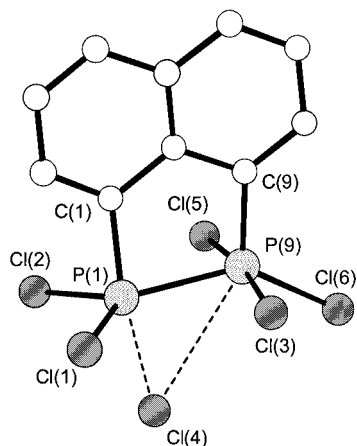


Figure 6. Calculated [B3LYP/6-31G(d,p)] transition state structure for the conversion of **2** to **3** (H atoms omitted for clarity); selected bond lengths [Å] and angles [°] P(1)–P(9) 2.256, Cl(4)–P(1) 2.460, Cl(4)–P(9) 2.970, P(1)–Cl(4)–P(9) 67.0

By analogy with $\text{P}(\text{CH}_2\text{Cl})\text{Cl}_4$, which has $\delta_{\text{P}} = -39.0$ ppm for the pseudo-trigonal bipyramidal structure (in solution),^[9] we anticipate a similar chemical shift in **3**. Not surprisingly, given the inequality in the populations of **2** and **3** suggested by our calculations, separated signals were not observed in the 121.4 MHz ^{31}P NMR spectrum at any temperature studied (193–373 K). However, changes were observed in linewidth, $^1J_{\text{P,P}}$ and δ_{P} , which is consistent with a dominant population (namely **2**) being in exchange on the NMR timescale with a second minor population (namely **3**) at higher temperatures. The observed increase of $^1J_{\text{P,P}}$ with increasing temperature probably reflects an increasing population of **3** (where a shorter P–P bond is found) with increasing temperature. Note that in **3**, the two phosphorus centres are not necessarily magnetically equivalent. The degree of inequivalence depends on the rate of ligand exchange (a process similar to pseudorotation), which is necessarily a concerted process in the sterically overcrowded environment. The presence of an ionic-molecular equilibrium would suggest substantial solvent-dependence of $^1J_{\text{P,P}}$. The magnitude of $^1J_{\text{P,P}}$ at 273 K, determined from the 121.4 MHz ^{31}P NMR spectra, is 131 Hz in $[\text{D}_8]\text{toluene}$ solution and 100 Hz in $[\text{D}_2]\text{dichloromethane}$ solution. Thus, the less-polar solvent (toluene) shifts the equilibrium to the molecular form **3**.

Conclusion

NapP_2S_4 (**1**) was used previously as a source of the NapP_2 moiety in many reactions with nucleophiles, though generally P–S–P bridge or P=S moieties were retained in their products. In this paper we have shown that **1** can be completely desulfurated in the reaction with chlorine gas, giving NapP_2Cl_6 (**2**). In analogy to PCl_5 or PhPCl_4 , **2** is expected to allow access to new main-group derivatives of 1,8-P,P-naphthalene with interesting bonding and chemistry. NMR spectroscopic data and calculations suggest that

the dynamic process observed in solutions of **2** might be explained by interchange between the ionic phosphonium-phosphoride form **2** and the molecular bis(phosphorane) form **3**; an intramolecular equivalent to the dynamic equilibrium of ionic $[\text{PCl}_4][\text{PCl}_6]$ and molecular PCl_5 forms.

Experimental Section

General Remarks: All manipulations were performed using standard Schlenk techniques with carefully dried and deoxygenated solvents under an oxygen-free argon atmosphere. Compound **1** was prepared as described previously.^[17] NMR: Varian Unity Plus 500, Bruker AM 300 and Jeol GSX 270; Ra: Perkin–Elmer System 2000. MS: VG Autospec.

NapP_2Cl_6 (2**):** Chlorine gas was bubbled through an externally cooled (0 °C), vigorously stirred suspension of **1** (14.3 g, 45.2 mmol) in dichloromethane (90 cm³). The reaction was completed after ca. 10 min, during which time the solid dissolved completely, and a new yellow solid (**2**) precipitated. The product was collected by filtration, washed with dichloromethane (30 cm³) and dried in vacuo. PCl_5 and further volatile by-products were sublimed off at 120–130 °C in vacuo (≈ 13 Pa). The remaining solid was of sufficient purity for further synthetic use, although its ^{31}P NMR spectrum (in THF, –30 °C, external lock) showed the presence of small amounts of partially oxidized/hydrolysed by-products. These impurities can be removed by twofold recrystallisation from hot THF. Yield after twofold recrystallisation 3.60 g (20%) of **2** in the form of yellow, extremely moisture sensitive crystals. Compound **2** is barely soluble in cold dichloromethane and toluene, but more soluble in THF. The crystals used for X-ray work were obtained from hot toluene. M.p. 208–211 °C with gas evolution. ^1H NMR (500 MHz, CD_2Cl_2 , 258 K, TMS): $\delta = 7.75$ [m, 1 H, H(3)], 7.95 [t, $^3J_{\text{H,H}} = ^3J_{\text{H,P}} = 7.7$ Hz, 1 H, H(8)], 8.02 [t, $^3J_{\text{H,H}} \approx ^4J_{\text{H,H}} \approx 6.0$ Hz, 1 H, H(4)], 8.42–8.50 [m (overlapped), 2 H, H(6) and H(7)], 8.76 [dd, $^3J_{\text{H,P}} = 33.1$, $^3J_{\text{H,H}} = 7.6$ Hz, 1 H, H(2)] ppm. $^{13}\text{C}\{^1\text{H}\}$ (125.7 MHz, $[\text{D}_8]\text{THF}$, 258 K, TMS), only signals of tertiary carbons could be assigned as the solubility of **2** at low temperatures was very low: $\delta = 124.9$ [t (virtual), $^2J_{\text{C,P}} \approx 14.1$ Hz, C(2)], 129.9–129.5 [m (overlapped), C(8) and C(3)], 131.8 [s, C(4)], 135.6 [s, C(7)], 140.7 [s; C(6)] ppm. $^{31}\text{P}\{^1\text{H}\}$ (121.4 MHz, CD_2Cl_2 , external reference 85% H_3PO_4 , for numbering of atoms see Figure 1): at 298 K 2 \times broad d (AX system), $\delta_{\text{P}} -225.4$ [P(9)] and 83.2 [P(1)], $^1J_{\text{P,P}} = 105.7$ Hz; at 223 K 2 \times d (AX system), $\delta_{\text{P}} -227.9$ [P(9)] and 82.2 [P(1)], $^1J_{\text{P,P}} = 83.8$ Hz. Raman (sealed capillary): $\tilde{\nu} = 3068$ (s, Ar–H), 1556 (s), 1365 (s), 435 and 420 (m, P–Cl), 322 cm^{–1} (vs). MS (EI+, 70 eV, sampled neat): $m/z = 365$ [M – Cl], 330 [M – 2Cl], 293 [M – 3Cl, base peak].

Computational Methodology: All calculations were performed on a dual processor Silicon Graphics Octane² Workstation. Initial guess structures were constructed using Maestro (Version 3.0.r38) and computations were carried out using Jaguar (Version 4.1.r53).^[18] The identity of ground and transition states was verified by vibrational frequency analysis and the calculated transition state possessed one imaginary vibration which corresponded to the reaction coordinate.

X-ray Crystallographic Study: Crystal data for **2**: $\text{C}_{10}\text{H}_6\text{Cl}_6\text{P}_2$, mol. wt. 400.8, yellow plates, $0.1 \times 0.1 \times 0.1$ mm, monoclinic, space group $P2_1/n$, $Z = 4$, $a = 8.1613(9)$, $b = 18.053(2)$, $c = 10.0490(9)$ Å, $\beta = 97.197(3)^\circ$, $V = 1468.9(3)$ Å³, $\rho_{\text{calcd.}}$ 1.363 Mg·m^{–3}, $2\theta_{\text{max}} = 46.46^\circ$, graphite monochromated Mo- K_α radiation ($\lambda = 0.71073$

\AA), $\mu(\text{Mo-K}\alpha) = 1.363 \text{ mm}^{-1}$, $T = 293 \text{ K}$. Data were measured on a Bruker SMART CCD, and Lorentzian polarisation and absorption (SADABS, max./min. transmission 1.0000/0.7767) corrections were performed. Of 6227 measured data, 2085 were unique and 1706 observed [$I > 2\sigma(I)$]. The structure was solved by direct methods. The non-hydrogen atoms were refined anisotropically, the hydrogen atoms were idealised and refined isotropically using a riding model. Structural refinements were performed with the full-matrix least-squares method on F^2 using the program SHELXTL (Version 5.10, Bruker AXS, 1997) to give $R_1 = 0.0438$ and $wR_2 = 0.1114$, with a residual electron density of $0.82 \text{ e}\text{\AA}^{-3}$.

CCDC-182100 contains the supplementary crystallographic data for **2**. These data can be obtained free of charge at www.ccdc.cam.ac.uk/conts/retrieving.html [or from the Cambridge Crystallographic Data Centre, 12, Union Road, Cambridge CB2 1EZ, UK; Fax: (internat.) +44-1223/336-033; E-mail: deposit@ccdc.cam.ac.uk].

Acknowledgments

We thank the EPSRC for funding.

- [¹] M. R. St. J. Foreman, J. D. Woollins, *J. Chem. Soc., Dalton Trans.* **2000**, 1533–1543.
 [²] P. Kilian, A. M. Z. Slawin, J. D. Woollins, *Eur. J. Inorg. Chem.* **1999**, 2327–2333.
 [³] P. Kilian, J. Marek, R. Marek, J. Tousek, O. Humpa, A. M. Z. Slawin, J. Touzin, J. Novosad, J. D. Woollins, *J. Chem. Soc., Dalton Trans.* **1999**, 2231–2236.

- [⁴] A. Karacar, H. Thonnessen, P. G. Jones, R. Bartsch, R. Schmutzler, *Chem. Ber./Recueil* **1997**, *130*, 1485–1489.
 [⁵] A. Karacar, M. Freytag, H. Thonnessen, P. G. Jones, R. Bartsch, R. Schmutzler, *J. Organomet. Chem.* **2002**, 643–644, 68–80.
 [⁶] A. Karacar, V. Klaukien, M. Freytag, H. Thonnessen, J. Omelanczuk, P. G. Jones, R. Bartsch, R. Schmutzler, *Z. Anorg. Allg. Chem.* **2001**, 627, 2589–2603.
 [⁷] D. Schomburg, *Acta Crystallogr., Sect. A* **1984**, *40*, C265.
 [⁸] M. Sanchez, R. Reau, F. Dahan, M. Regitz, G. Bertrand, *Angew. Chem.* **1996**, *108*, 2386–2388; *Angew. Chem. Int. Ed. Engl.* **1996**, *35*, 2228–2230.
 [⁹] K. B. Dillon, T. A. Straw, *J. Chem. Soc., Chem. Commun.* **1991**, 234–235.
 [¹⁰] H. Luo, R. McDonald, R. G. Cavell, *Angew. Chem.* **1998**, *110*, 1172–1174; *Angew. Chem. Int. Ed.* **1998**, *37*, 1098–1099.
 [¹¹] M. Sanchez, R. Reau, H. Gornitzka, F. Dahan, M. Regitz, G. Bertrand, *J. Am. Chem. Soc.* **1997**, *119*, 9720–9728.
 [¹²] W. S. Sheldrick, J. A. Gibson, G.-V. Roschenthaler, *Z. Naturforsch., Teil B* **1978**, *33*, 1102–1105.
 [¹³] C. W. Schultz, R. W. Rudolph, *J. Am. Chem. Soc.* **1971**, *93*, 1898–1903.
 [¹⁴] H. W. Roesky, D. Amirzadeh-Asl, W. S. Sheldrick, *J. Am. Chem. Soc.* **1982**, *104*, 2919–2920.
 [¹⁵] J. E. Richman, R. O. Day, R. R. Holmes, *Inorg. Chem.* **1981**, *20*, 3378–3381.
 [¹⁶] J. E. Richman, R. O. Day, R. R. Holmes, *J. Am. Chem. Soc.* **1980**, *102*, 3955.
 [¹⁷] M. R. St. J. Foreman, J. Novosad, A. M. Z. Slawin, J. D. Woollins, *J. Chem. Soc., Dalton Trans.* **1997**, 1347–1350.
 [¹⁸] Schrodinger Inc., Portland, Or, USA, 2001.

Received June 11, 2002
 [I02308]